Modeling the Spread of a Pathogen over a Spatially Heterogeneous Growing Crop

J.B. Burie, M. Langlais
Université de Bordeaux, IMB, UMR 5251, F-33076 Bordeaux, France
CNRS, IMB, UMR 5251, F-33400 Talence, France

A. Calonnec
INRA, UMR1065 SAVE, F-33883 Villenave d'Ornon, France
Université de Bordeaux, ISVV, UMR SAVE, F-33883 Villenave d'Ornon, France

Y. Mammeri*
LAMFA - CNRS UMR 7352, Université de Picardie Jules Verne, 80039 Amiens, France
*Corresponding author.
e-mail: youcef.mammeri@u-picardie.fr

***Abstract*— The spread of a pathogen within an anthropized crop plot depends on many factors acting at contrasted spatio-temporal scales. This is of paramount importance for vine and powdery mildew, one of its airborne pathogen. We aimed at developing a coupled PDEs-ODEs model for plant-pathogen interactions at the plot scale level in order to assess the effects of various host heterogeneities on the epidemic spread.**

Keywords-component; plant-pathogen; heterogeneous plot; PDE-ODE; simulations.

I. INTRODUCTION

Current strategies for crop protection generate complex and controversial issues both on the human health and the environment. Growers are now constrained to significantly reduce the use of fungicides (Directive 1107/2209/ EU). However, up to now, because of the important efficiency of these fungicides at reducing epidemics, systems based on the development of innovative control methods have not been much developed and evaluated.

Modeling is a key approach to improve the understanding of host/pathogen dynamical interactions, to rank known factors that initiate the development of an epidemic and to test strategies to control and reduce its spread. In the powdery mildew/grapevine pathosystem, we hypothesized that dynamical changes in crop structure and susceptibility should be considered as key factors for explaining variability in the severity of epidemic behavior ([1; 2]).

We therefore devised epidemiological simulation models coupling grapevine growth with the dispersal and disease dynamics of the pathogen, to evaluate the ability of the host development to modify fungal epidemics.

The first model we developed was a complex discrete mechanistic architectural model at the plant scale that explicitly incorporates both the host growth and the development and dispersion of the pathogen [1]. The model strengthens observed experimental results about the effects of the rate of leaf emergence and of the number of leaves at flowering on the severity of the disease [3]. But it also underlines strong variations of the dynamics of the disease depending on the vigour and indirectly on the climatic scenarios by altering the synchronism between the disease and the production of susceptible organs.

The second model was a compartmental SEIRT model at the plant scale based on a system of ordinary differential equations (ODEs). Host growth is handled as a logistic increase of the foliar surface before and after shoot topping. The ontogenic resistance of the leaves is also taken into account. In [4], we investigated the ability of this mathematical model to retrieve the main dynamics of the disease for several vine growth scenarios. Using the outputs of the discrete model to calibrate the parameters of the SEIRT model, the host growth and the disease development was correctly reproduced with a small computing time compared to the discrete one.

Extension of the ODEs SEIRT model at the plot scale is more straightforward than that of the discrete one. In this work we shall devise a Reaction-Diffusion system at the plot scale coupled to ODEs at the plant scale.

A partial differential equations (PDEs) model for a homogeneous plot was introduced in [5] to study the influence of a dual dispersal mechanism (short range and long range dispersal of spores) on the disease propagation. In Burie et al. [6], we showed that the row structure of vineyards had an influence on the disease spatial spread. The PDEs model considered there was devised from a rather qualitative point of view and was somewhat lacking biological realism. Typically, experimental results in [3] indicate that the speed of propagation of the disease is higher along the direction perpendicular to rows than along rows, a contradiction to numerical experimentations from [6].

In this work, we shall improve the realism of the model in [6] by adding a finer description of the spore dispersal process and also by using more biologically relevant parameters. Then, using numerical simulations one shall explore the influence of heterogeneities within the plot and the plant (e.g. vigour) and between plots (e. g. phenology, density of plantation, spatial organization) on the epidemics development, and also

978-1-4673-0070-4/12/$31.00 ©2012 IEEE

the influence of the density of the initial inoculums. Finally, we shall include the description of fungicide treatments in the model and test the impact of the treatment timings on the epidemic.

In the following, we will first present the model and briefly outline some of its mathematical qualitative properties (Section II). Then through numerical experiments we shall explore the evolution of the disease according to the climate and the vigour for heterogeneous plots. A first approach of the use of fungicides is introduced (Section III).

II. Model Description

A model for the interaction of powdery mildew and vine growth at a single plant scale has been proposed in [1]. It describes the plant architecture accurately, as well as the spread of the pathogen. This very detailed model takes into account the 3D development of each organ and each infectious event.

At the plot scale the number of plants becomes too large to describe in detail each event. Devising an architectural model for each plant would require a huge computational time. An alternative approach is to use a continuous model for the leave surface or for the density of leaves, i.e. the leaf surface area per unit of ground surface (also called leaf area index), with respect to its epidemiological state and its location in the plot. One could also consider the leave density per area of volume. For a single plant, Burie et al. [4] proposed a system of ordinary differential equations of SLIRT type (Sensitive, Latent, Infectious, Removed, ontogenic resisTant) .

One shall devise a SLIRT system of ODEs describing the evolution of the leave density coupled with a system of PDEs describing the spread of spores. This is an improved version of [6] that includes new features considered in [4] at the plant scale, i.e. ontogenic resistance (age-related resistance) and shoot topping. Moreover, the spore dispersal description has been refined to take into account a barrier effect due to the leaves. This barrier effect could explain that the disease propagation speed is lower along vine rows than across rows. The model also allows considering heterogeneous plots in space (variation of growth, of phenology and of crop structure), with some agricultural practices occasionally dependent of space and time.

Overall, the model is an improved combination of models in [1], [4] and [6] to which we refer for additional details.

A. Modeling

The development of a powdery mildew epidemic at the plot scale requires taking into account the spore dispersal between plants. The disease cycle is the following (see Figure 1 for a schematic representation of the model): susceptible leaves (denoted by S) inoculated with spores first become latent (L), then turn infectious (I) and produce spores during some infectious period after which they are removed (R) as they cannot be infected again. In addition, susceptible leaves become resistant to inoculation because of their age (T).

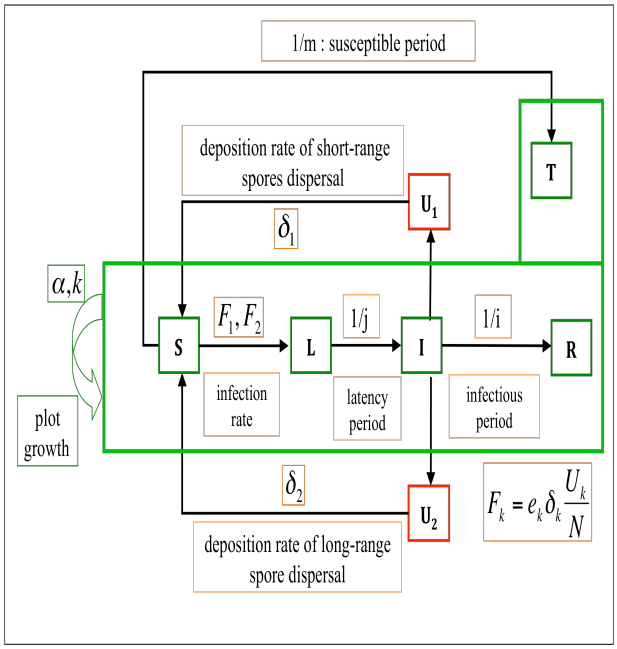

Figure 1. Flow chart of the model system.

The total density of leaves is,

$$N = S + L + I + R + T.$$

The disease has no significant impact on the plant growth. Thus one assumes a logistic growth,

$$\frac{d}{dt}N(x,t) = \alpha(x,t)N(x,t)\left(1 - \frac{N(x,t)}{k(x,t)}\right),$$

with parameters $\alpha > 0$ and $k > 0$. These coefficients depend on the spatial location x and can be impacted by agricultural practices such as shoot topping. Shoot topping will first suppress part of the leaves and then induce a sudden change of the growth rate of the plant. Hence, we set

$$\alpha(x,t) = \begin{cases} \alpha_0(x) \text{ before shoot topping} \\ \alpha_1(x) \text{ after shoot topping,} \end{cases}$$

$$k(x,t) = \begin{cases} k_0(x) \text{ before shoot topping} \\ k_1(x) \text{ after shoot topping.} \end{cases}$$

The airborne spores densities (with respect to ground unit) are structured according to their range of dispersal, short ranged spores density is denoted by U_S and long ranged one by U_L.
This leads to the following ODEs system for leaves, parameterized by x in some spatial domain Ω,

$$\frac{d}{dt}S(x,t) = -\left(e_S\delta_S U_S(x,t) + e_L\delta_L U_L(x,t)\right)\frac{S(x,t)}{N(x,t)} + \alpha N(x,t)\left(1-\frac{N(x,t)}{k}\right) - \frac{1}{m}S(x,t)$$

$$\frac{d}{dt}L(x,t) = \left(e_S\delta_S U_S(x,t) + e_L\delta_L U_L(x,t)\right)\frac{S(x,t)}{N(x,t)} - \frac{1}{j}L(x,t)$$

$$\frac{d}{dt}I(x,t) = \frac{1}{j}L(x,t) - \frac{1}{i}I(x,t)$$

$$\frac{d}{dt}R(x,t) = \frac{1}{i}I(x,t)$$

$$\frac{d}{dt}T(x,t) = \frac{1}{m}S(x,t).$$

Airborne spores land on plants at short range and long-range deposition rates $\delta_S > 0$ and $\delta_L > 0$. Due to their longer air borne transportation time and to the reduction of spore viability due to UV, long-range spores have a smaller efficiency of infection than the short-range ones, i.e. $0 < e_L < e_S$.

Partial differential equations are used to describe the airborne dispersal of the pathogen, [5,6].
Spores are torn off from a colony of fungus by wind gusts. Spores are produced by infectious leaves at a rate $\gamma > 0$. Each emitted spore has a probability $f(N) \in [0,1]$ to be of short-range type and thus a probability $(1 - f(N))$ to be of long-range type.
Spores move according to a Fick's law diffusion with diffusion coefficients $D_L > D_S > 0$. For long range ones the action of dominating winds is taken into account by adding a convection term with velocity V.
Dispersal parameters, diffusion coefficients as well as deposition rates, depend on the total leave density N as one expects the spore dispersal to be more difficult when the leave density is larger. This yields a model system,

$$\partial_t U_S(x,t) = \nabla.\left(D_S(N)\nabla U_S(x,t)\right) - \delta_S U_S(x,t) + \gamma f(N) I(x,t)$$

$$\partial_t U_L(x,t) = \nabla.\left(D_L(N)\nabla U_L(x,t)\right) - V(x,t).\nabla U_L(x,t) - \delta_L U_L(x,t) + \gamma\left(1-f(N)\right)I(x,t).$$

This model system is supplemented with initial conditions S^0, L^0, I^0, R^0, T^0 and U_s^0, U_l^0. Homogeneous Dirichlet boundary conditions are assigned for U_S and U_L on the boundary of a much larger spatial domain than the crop plot, Ω, at hand, see [6]. At shoot topping (removal of leaves) another set of initial conditions has to be given.
As in [6], the row structure of the plot is handled by setting $N=S=L=I=R=T=0$ for x corresponding to any location outside rows. As a consequence plant densities as well as dispersal parameters are spatially discontinuous functions in general.

Finally, fungicide treatments are modelled by altering coefficients linked with the infection (e_S and e_L) for some duration, and/or the sporulation rate (γ) depending on the fungicide type.

B. *Qualitative properties*

From a mathematical analysis point of view, the first thing to be checked is the well posedness of the model system that is the model system possesses a unique component wise nonnegative solution defined for all time. This can be achieved through lengthy calculations, see [7].

As in [6], one can look for the long-term behaviour of the solution. As time goes to infinity, (U_S,U_L,S,L,I,R,T) converges a.e. to $(0,0,0,0,0,R^*,T^*)$ with $R^*(x)+T^*(x)=k(x)$.

In the homogeneous case (all parameters independent of x) as in [4], due to the ontogenic resistance of the disease and the host growth, the leave density is not a constant and the proportion of susceptible density also varies. Therefore, instead of the basic reproduction number, we again consider the effective reproduction number and introduce,

$$R_{eff}(t) := i\gamma\left(e_s f(N(t)) + e_l(1-f(N(t)))\right)\frac{S(t)}{N(t)}.$$

In the heterogeneous case, this number depends on x. For the simulations (section 3.3), we will consider at the plot scale,

$$R_{plot}(t) = \frac{1}{Area(Plot)}\int_\Omega R_{eff}(x,t)dx.$$

III. NUMERICAL ISSUES

The architectural model describing the growth of one plant and the propagation of the pathogen within this plant and its porting on the Open Alea platform [1; 8] provides us with the following data:

1. The daily number of leaves with their age and epidemiological status, the amount of spores that propagate within the canopy and the amount that escapes. These data will allow us to calibrate the continuous model for each plant (see subsection III.B).

2. The percentage of surface of each type of leaves (*S, L, I, R* or *T*) cut at each cultural management event such as pruning or topping (see Table I).
3. The age and the geometry of each organ.

TABLE I. PERCENTAGE OF THE SURFACE OF SUSCEPTIBLE, LATENT, INFECTIOUS, REMOVED AND RESISTANT LEAVES CUT AT SHOOT TOPPING IN THE ARCHITECTURAL MODEL.

Year	Topping day	Inoculation day	%S	%L	%I	%R	%T
1998	169	115	70	7	5	62	14
	169	131	70	9	0	44	0.2

It takes an average time of half an hour for the airborne spores to fall over the plant. Hence we set the deposition rates to be

$$\delta_S = \delta_L = 50 \text{ day}^{-1}.$$

The standard deviation of the distribution of fallen spores emitted from a single source by the dispersal model is given by

$$\sigma = \sqrt{\frac{D}{\delta}}.$$

The diffusion coefficients are chosen in such a manner that the long-range dispersion is

$$\sigma_L = 20 \text{ m}, D_L = 20000 \text{ m}^2\text{day}^{-1},$$

and the short-range dispersion is

$$\sigma_S = 2 \text{ m}, D_S = 200 \text{ m}^2\text{day}^{-1}.$$

One vine stock covers a surface area of *0.4 m²* (width *50 cm* and length 80 *cm*), we have set the short distance dispersal coefficients so that that the spores disperse within the vine stock.

A barrier effect is taken into account for the short-range dispersal: the diffusion decreases with leaves density. The expression of this diffusion function is not clear; we will perform several tests with a logarithmic, polynomial or exponential decay. We then choose coefficients following [9; 10]: for x ∈ Ω and t > 0,

$$D_S(N) = 200, \ \frac{200}{1+\log(1+N)}, \ \frac{200}{1+N^2} \text{ or } 200\exp(-N^2),$$

$$D_L(N) = 20000,$$

$$f\big(N(x,t)\big) = N(x,t)/\big(1+N(x,t)\big).$$

A. Time and space discretizations

We consider a semi-implicit scheme for the time discretization. Let $\Delta t > 0$ be the time step and set,

$$Y^n(x) = Y(x, n\Delta t).$$

Our numerical scheme reads as follows.

$$U_S^{n+1} = U_S^n + \Delta t \left[\nabla.\left(D_S(N^{n+1})\nabla U_S^{n+1}\right) - \delta_S U_S^n + \gamma f(N^n) I^n\right]$$

$$U_L^{n+1} = U_L^n + \Delta t \left[\nabla.\left(D_L(N^{n+1})\nabla U_L^{n+1}\right) - \delta_L U_L^n - V^n.\nabla U_L^n + \gamma(1 - f(N^n)) I^n\right]$$

$$S^{n+1} = S^n + \Delta t \left[-\left(e_S\delta_S U_S^n + e_L\delta_L U_L^n\right)\frac{S^n}{N^n} + \alpha N^n\left(1 - \frac{N^n}{k}\right) - \frac{1}{m}S^n\right]$$

$$L^{n+1} = L^n + \Delta t \left[\left(e_S\delta_S U_S^n + e_L\delta_L U_L^n\right)\frac{S^n}{N^n} - \frac{1}{j}L^n\right]$$

$$I^{n+1} = I^n + \Delta t\left[\frac{1}{j}L^{n+1} - \frac{1}{i}I^n\right]$$

$$R^{n+1} = R^n + \frac{\Delta t}{i}I^{n+1}$$

$$T^{n+1} = T^n + \frac{\Delta t}{m}S^{n+1}.$$

For spatial discretization, we use a second order splitting method to separate the advection-reaction-diffusion equations into an elliptic part and a transport one. A finite volume method is used to solve the elliptic equation, [11]. On the other hand, the transport equation is dealt with a WENO5 scheme, [12].

In each case, a Cartesian grid of the spatial domain is chosen. The length and width of the computational domain are three times larger than those of the plot, see [6].

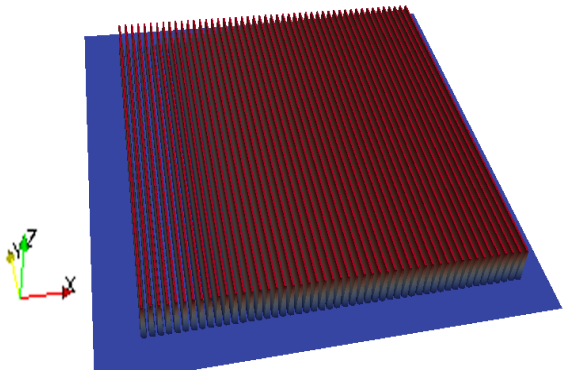

Figure 2. Simulated plot.

Remark 3.1: Qualitative behavior of continuous solutions have to be preserved by the discrete solution given by the numerical method.

1. The plot is made of rows of plants. Outside of these rows there is no plant and our numerical method allows keeping the density of leaves at zero there (see Figure 2). The finite volume method is well adapted to handle piecewise discontinuous diffusion coefficients, [11].

2. As in the continuous case (subsection II.B), the approximate solution remains nonnegative.
3. Simulations are performed with Dirichlet boundary conditions. To reduce the impact of reflections at the boundaries of the domain, we used a computational domain in which the distance between the plot and the boundary of the domain is large enough. More realistic boundary conditions, such as absorbing ones, could be used to take into account the output and input of spores in the domain.

B. Calibration at the plant scale

The architectural model provides daily data for the density of susceptible (age less than *m* days) (S_A), latent (L_A), infectious (I_A) and removed leaves (R_A) at the plant scale. The amount of spores propagating inside the plant as well as of those outgoing from the plant is also available, giving $U_{S;A}$ and $U_{L;A}$ respectively. We aim to minimize the functional,

$$\begin{aligned} J(\theta) &= \frac{1}{2}\sum_{t=0}^{T} \| Y(\theta,t) - Y_A(t) \|^2_{L^2(\Omega)} \\ &= \frac{1}{2}\sum_{t=0}^{T}\int_{\Omega} \left(Y(\theta,t) - Y_A(t)\right)^2 dx, \end{aligned}$$

where Y is a solution to the system,

$$\begin{aligned} \partial_t Y &= F(x,t,Y,\nabla Y,\theta) \\ Y(t=0) &= Y_0, \end{aligned}$$

Y_A is the output of the architectural model and $\theta = (\gamma, \alpha, k)$ are the model parameters to be calibrated. Other parameters are fixed for this work.

The minimum of J is achieved when its gradient vanishes. This gradient reads,

$$\nabla J(\theta) = \sum_{t=0}^{T}\int_{\Omega} \left(\frac{\partial F(x,t,Y,\theta)}{\partial \theta}\right)^t \lambda(x,t)\,dx$$

wherein λ is a solution to the backward system of partial differential equations,

$$-\partial_t \lambda = \left(\frac{\partial F(x,t,Y,\theta)}{\partial Y}\right)^t \lambda(x,t) + (Y - Y_A),$$

for t in [0,T], with the final condition at t=T,

$$\lambda = (\lambda_1,\lambda_2,\lambda_3,\lambda_4,\lambda_5,\lambda_6,\lambda_7)(t=T) = 0.$$

One can show λ is a solution of an adjoint problem, a backward system made of five ODEs and two PDEs quite similar to the original (primal) one. The same discretization is used to perform the simulation of the adjoint problem.

Algorithm:

While $||\nabla J(\theta^m)|| \geq \varepsilon$ or $m \leq M_{max}$ **do**

1. **Solve** the primal problem $Y^m(x,t,\theta^m)$.
2. **Solve** the adjoint problem $\lambda^m(x,t,\theta^m)$.
3. **Solve** the gradient: for

$$\theta^{m+1} = \theta^m - \rho_m \left(\frac{\partial F}{\partial \theta^m}\right)^t \lambda^m.$$

end while

The model simulation starts at the day of primary infection. At shoot topping the various compartments of leave densities are updated to take into account the amount of foliar surface cut (see Tables III and IV).

In Table II and Figure 3, we present some results obtained with the above procedure for year 1998. The simulations start at day 115 with

$$S^0 = 15,\ L^0 = 25,$$

$$I^0 = R^0 = T^0 = U_S^0 = U_L^0 = 0.$$

Simulations presented here are performed for a plot made of one single plant, i.e. a row of width *0.5 m* and length *0.8 m* with steps $\Delta x = \Delta y = 0.1$, $\Delta t = 0.01$. We choose,

$$\delta_S = \delta_L = 50,\ e_S = 0.01,\ e_L = 0.005,\ i = j = m = 10$$

$$D_S(N) = 200$$

$$D_L(N) = 20000.$$

The rate of host growth (α), the carrying capacity (k) and production rate of spores (γ) are approximated with the above algorithm.

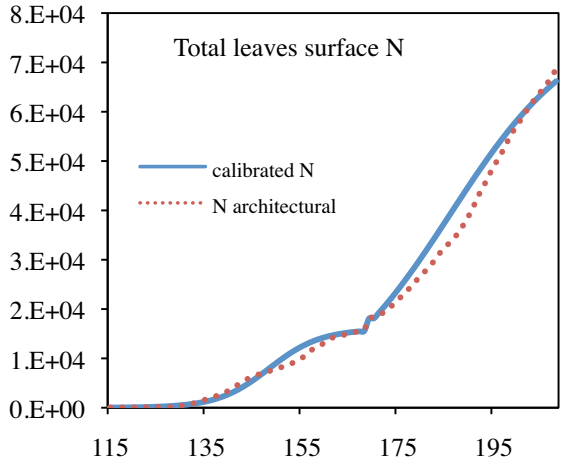

Figure 3. Evolution of the total leave surface area (cm²) with respect to day simulated by the architectural model (N_a) and the PDE model (N), before and after shoot topping for the year *1998* and vigour *1* for early inoculation at the vine level.

TABLE II. ESTIMATED PARAMETERS OF THE RATE OF HOST GROWTH (α), THE CARRYING CAPACITY (K) AND PRODUCTION RATE OF SPORES (γ).

Year	Vigour	Inoculation day	Before shoot topping		
			α	k	γ
1998	1	115	0.77	15944	742
			After shoot topping		
			α	k	γ
			0.073	78748	905

Simulations with different levels of vigour, various climates and agricultural practices, will allow us to set simulations at the plot scale. This plot will be composed of plants whose individual dynamics are similar to the ones of the architectural model.

Remark 3.2: Other parameters, namely (D_S, D_L, $f(N)$, e_S, e_L), difficult to determine from the experiments or from the architectural model, can be calibrated using this kind of method.

C. *Numerical simulations at the plot scale*

Simulations start at day of primary inoculation. We therefore start with $I^0 = R^0 = U_S^0 = U_L^0 = 0$. Other initial data are given by outputs of the architectural model (see Table III).

TABLE III. INITIAL DATA FOR THE INOCULATION SOURCE.

Year	Inoculation day	S^0	L^0	T^0
1998	115	15	25	0
	131	444	20	151

TABLE IV. INITIAL COEFFICIENTS ACCORDING TO VIGOUR.

Year	Vigour	Before shoot topping		After shoot topping	
		α	k	α	k
1998	1	0.17	15000	0.05	80000
	0.6	0.17	15000	0.02	50000
	0.2	0.17	15000	0.003	16000

Simulations presented here are performed with a plot composed of 50 rows of width *0.5 m* and length 98.*4 m* with *1.5 m* inter-rows. The number of plants per row is 123, making a total of 6150. We then define the computational domain as *[0, 295.5] x [0, 295.2]*, and steps $\Delta x = \Delta y = 0.1$, $\Delta t = 0.01$ until the 241th day. Here the infection starts at the plot center and we choose

$$\delta_S = \delta_L = 50,\ e_S = 0.01,\ e_L = 0.005,\ i = j = m = 10$$

$$D_S(N) = \frac{200}{1+N^2}$$

$$D_L(N) = 20000.$$

Figure 4 shows numerical results obtained for the year 1998 with three levels of vigour 1, 0.6 and 0.2 for the whole plots. Simulations at the plot scale are presented in Figure 6. The diseased surface density is defined by M=L+I+R.

As for the architectural model, the development of the disease depends on the plant vigour, the greater the vigour the greater the disease. This is well illustrated by the computation of the effective reproduction number at the plot scale R_{plot}, (see section II), which gives a synthetic view of the relationship between host growth and the disease. R_{plot} decreases during the growing season but can rise up after shoot topping when the vigour is high with an increase rate of secondary shoots development.

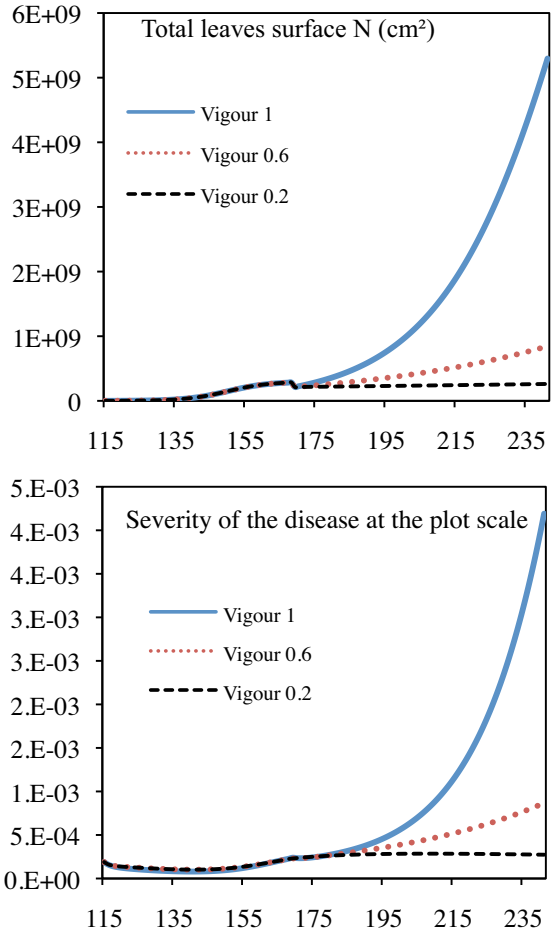

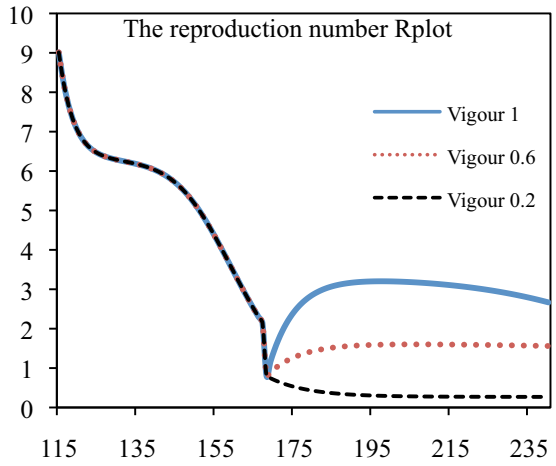

Figure 4. Evolution of the total leaf surface area (*N*), diseased surface area (*M*), and the effective reproductive number (R_{plot}) with respect to day simulated by the PDE model, for the year *1998* and three levels of vigour *(1, 0.6, 0.2)* for early inoculation *(day 115),* for the whole plot.

To take into account the use of fungicides, we decrease infection efficiency and sporulation rate during the 10 days that follow the fungicide application. Two strategies are tested: a fungicide application 10 days before shoot topping (around flowering time) and an application at shoot topping (Figure 5).

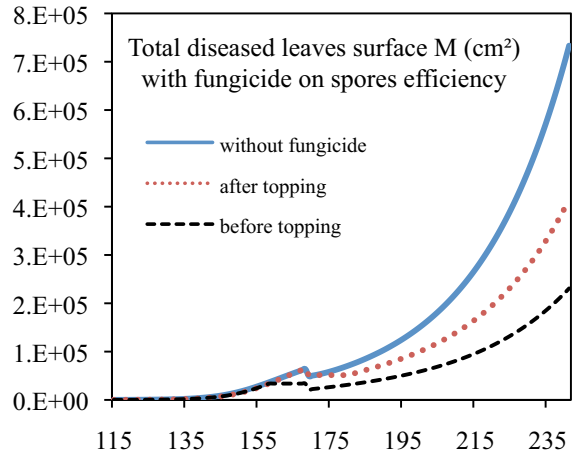

Figure 5. Evolution of the total diseased surface area (*M)* with respect to day depending on the application of one fungicide, simulated by the PDE model for the climatic scenario *1998*, vigour 0.6 and for early inoculation *(day 115)*, for a fungicide application 10 days before shoot topping or 10 days after shoot topping.

From the results, it seems that it is more efficient to use the fungicide just before the shoot topping.

Remark 3.3: Other simulations can be performed with:

1. Variation of the size of rows and inter-rows.
2. Heterogeneous patches of various vigours and phenology.
3. Plots with different locations of primary inoculum sources.

IV. Conclusion

The model proposed in this paper is a further step towards a realistic description of plant-pathogen interactions at the plot scale. Taking into account heterogeneous plots as well as climate and agricultural practices can perform relevant simulations. Various heterogenities on plot can be designed to estimate their influence on the epidemics propagation. In a future work, we plan to do a further comparison with experiments and a sensitivity analysis.

On the other hand, the numerical method allows using varying infection parameters. Then evaluation of control methods for the use of fungicides is made possible.

Acknowledgment

This study was supported by grants from the "Agence Nationale de la Recherche" programme SYSTERRA (ANR-08-STRA-04).

References

[1] A. Calonnec, P. Cartolaro, J.M. Naulin, D. Bailey, and M. Langlais, A host-pathogen simulation model: powdery mildew of grapevine. Plant Pathology 57 (2008) 493-508.

[2] H. Valdes-Gomez, C. Gary, P. Cartolaro, M. Lolas-Caneo, and A. Calonnec, Powdery mildew development is positively influenced by grapevine vegetative growth induced by different soil management strategies. Crop Protection 30 (2011) 1168-1177.

[3] A. Calonnec, P. Cartolaro, and J. Chadoeuf, Highlighting features of spatiotemporal spread of powdery mildew epidemics in the vineyard using statistical modeling on field experimental data. Phytopathology 99 (2009) 411-422.

[4] J.B. Burie, M. Langlais, and A. Calonnec, Switching from a mechanistic model to a continuous model to study at different scales the effect of vine growth on the dynamic of a powdery mildew epidemic. Annals of Botany 107 (2011) 885-895.

[5] M. Zawolek, and J.C. Zadoks, Studies in focus development: An optimum for the dual dispersal of plant pathogens. Phytopathology 82 (1992) 1288-1297.

[6] J.B. Burie, A. Calonnec, and M. Langlais, Modeling of the invasion of a fungal disease over a vineyard. Mathematical Modeling of Biological Systems. Series: Modeling and Simulation in Science, Engineering and Technology II (2007) 11-21.

[7] W.E. Fitzgibbon, M. Langlais, and J.J. Morgan, A mathematical model of the spread of Feline Leukemia Virus (FeLV) through a highly heterogeneous spatial domain, SIAM J. Math. Anal. 33 (2001) 570–588.

[8] C. Pradal, S. Dufour-Kowalski, F. Boudon, C. Fournier, and C. Godin, OpenAlea: A visual programming and component-based software platform for plant modeling. Functional Plant Biology 35 (2008) 751-760.

[9] D.E. Aylor, Biophysical scaling and the passive dispersal of fungus spores: relationship to integrated pest management strategies. Agricultural and Forest Meteorology 97 (1999) 275-292.

[10] A. Stockmarr, V. Andreasen, and H. Ostergard, Dispersal distances for airborne spores based on deposition rates and Stochastic Modeling. Phytopathology 97 (2007) 1325-1330.

[11] R. Eymard, T. Gallouet, and R. Herbin, Finite Volume Methods. in: P.G. Ciarlet, and J.L. Lions, (Eds.), Handbook of Numerical Analysis, 2007.

[12] G.S. Jiang, and C.W. Shu, Efficient implementation of weighted ENO schemes. J. of Computational Physics 126 (1996) 202-228.

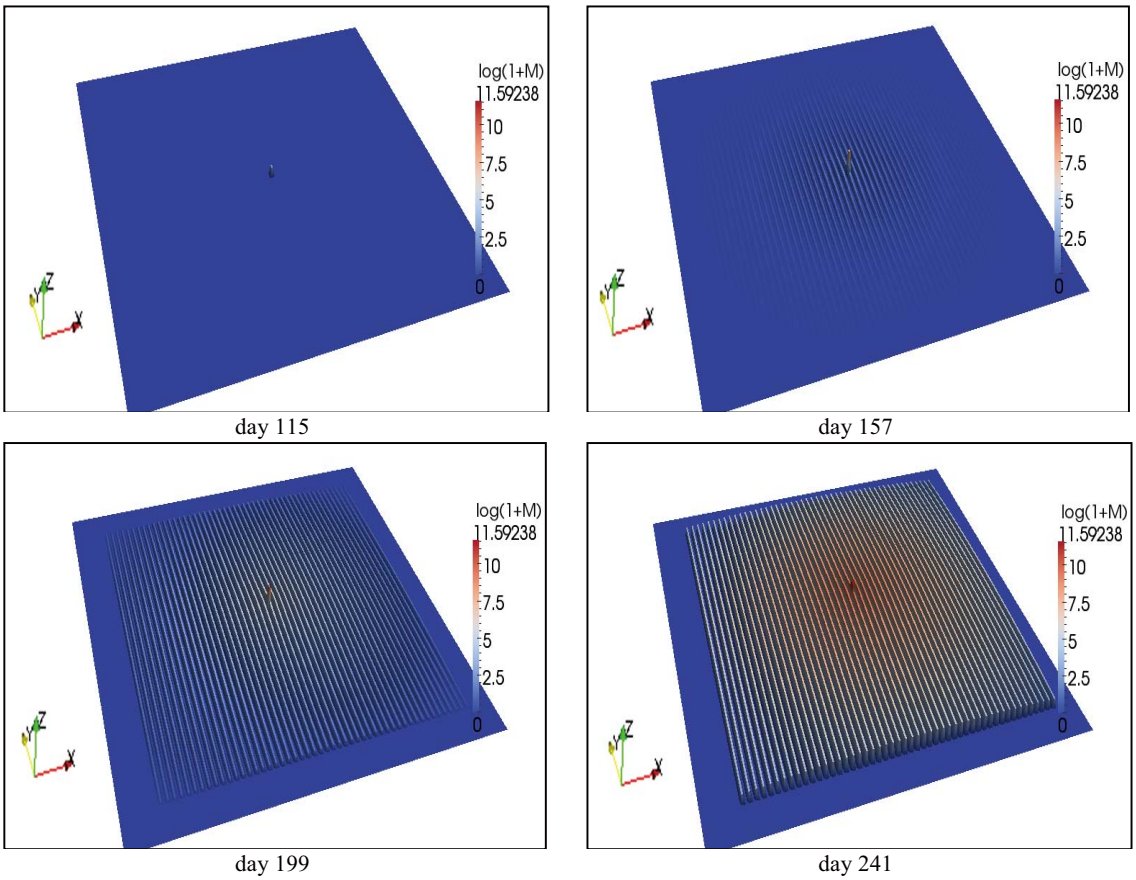

Figure 6. Evolution of the diseased area (M=L+I+R) at the plot scale with respect to day simulated by the PDE model, for the year 1998, vigor 1 and for early inoculation (day 115).